Stator Inter-Turn Fault Detection and Fault Tolerant Control in DTC Induction Motor Drives using an Extended Kalman Filter

Pracoviště: Regionální inovační centrum elektrotechniky
Číslo dokumentu: 22190-018-2022
Typ zprávy: Výzkumná zpráva
Řešitelé: Serge Pacome Bosson
Vedoucí projektu: Zdeněk Peroutka
Počet stran: 38
Datum vydání: 20.6.2022
Oborové zařazení: 2.2 Electrical engineering, Electronic engineering, Information engineering - Electrical and electronic engineering

Zadavatel / zákazník:

Zpracovatel / dodavatel:
Západočeská univerzita v Plzni
Regionální inovační centrum elektrotechniky
Univerzitní 8
306 14 Plzeň
Kontaktní osoba:
Serge Pacome Bosson
bosson@fel.zcu.cz

This research as been supported by the project No. SGS-2021-021

Anotace

Klíčová slova

Detekce chyb vinutí, PMSM, DTC, Extended Kalman Filter

Název zprávy v anglickém jazyce / Report title

Stator Inter-Turn Fault Detection and Fault Tolerant Control in DTC Induction Motor Drives using an Extended Kalman Filter

Anotace v anglickém jazyce / Abstract

This research report presents a fault detection model with fault tolerant control, that allow the system to continue operation in the presence of faults, for a stator inter-turn fault in DTC induction motor drives. The behaviour of a DTC drive in the presence of inter-turn short circuits is evaluated, which makes it possible to offer this technique for the detection of this type of fault. The fault detection is obtained by calculating a new fault indicator based on state and fault parameter estimation of the machine using an extended Kalman filter. Direct Torque Control (DTC) uses the stator resistance of the machine for the estimation of stator flux. The variation of stator resistance, due to stator winding turn fault, creates an error in the estimated stator flux and estimated electromagnetic torque. The fault tolerant control is obtained by estimating the stator resistance using the fault severity factor, estimated with the designed extended Kalman filter, to make the drive more robust and precise. The proposed model is simulated in Matlab/Simulink. The obtained simulation results show the effectiveness of the proposed technique.

Klíčová slova v anglickém jazyce / Keywords

Stator inter turn fault detection, fault tolerant control, DTC induction motor drives, Extended Kalman Filter.

Abstract

This research report presents a fault detection model with fault tolerant control, that allow the system to continue operation in the presence of faults, for a stator inter-turn fault in DTC induction motor drives. The behaviour of a DTC drive in the presence of inter-turn short circuits is evaluated, which makes it possible to offer this technique for the detection of this type of fault. The fault detection is obtained by calculating a new fault indicator based on state and fault parameter estimation of the machine using an extended Kalman filter. Direct Torque Control (DTC) uses the stator resistance of the machine for the estimation of stator flux. The variation of stator resistance, due to stator winding turn fault, creates an error in the estimated stator flux and estimated electromagnetic torque. The fault tolerant control is obtained by estimating the stator resistance using the fault severity factor, estimated with the designed extended Kalman filter, to make the drive more robust and precise. The proposed model is simulated in Matlab/Simulink. The obtained simulation results show the effectiveness of the proposed technique.

Keywords

Stator inter turn fault detection, fault tolerant control, DTC induction motor drives, Extended Kalman Filter.

List of symbols and shortcuts

GPS	Global Position System

Contents

1 Introduction

Stator inter-turn faults in three-phase induction machines (IM) account for about 40% of machine failures in industrial applications [1]. Significant research has been conducted for this type of defect, when the IM is connected directly online (DOL) to the grid [2]-[6]. However, it has been recognized that the techniques usually used for the diagnosis of faults in line-fed motors and in open-loop drives cannot be used straightforward when the motor is part of a more complex control structure, like the one found in modern closed-loop drives, based on Direct Torque Control (DTC) or Field Oriented Control (FOC) [7]. A lot of recent research, conducted in the field of fault diagnosis, has been focused on the diagnosis of inter turn faults in closed-loop induction motor drives [8]-[15].

In addition, within the category of closed-loop drives, it was also shown that systems based on Direct Torque Control and Field Oriented Control, under the presence of faults, exhibit different behaviours [7]. Indeed, the components present in these drives have a major impact on the way how the effects of the fault will appear in the motor drive variables [16]. In this context, there is a need to study more deeply the impact of the control system in the variables and quantities which may be used for diagnostic purposes. Among all the IM vector controllers, Direct Torque Control (DTC) is widely in use, nevertheless, it has been less researched than Field Oriented Control (FOC) for inter-turn fault. The extensive use of direct torque control (DTC) induction motor drives nowadays motivates the study of the occurrence of stator faults in this type of system as well.

On the other hand, fault-tolerant control (FTC) has attracted increasing attention in the last two decades in applications, where keeping the continuation of operation is the paramount requirement [17]. For safety-critical applications, such as electric vehicles, industrial applications, maintaining minimum machine operation after failure is much better and safer than immediate machine shutdown. It is known that the occurrence of a fault can degrade the control performances and in some cases lead to the instability of the system. Consequently, many strategy for fault-tolerant control (FTC) are introduced to tolerate the fault effect and maintain system stability [18]. In literature, we find two approaches for the design of fault-tolerant control: passive fault-tolerant control (PFTC) and active fault-tolerant control (AFTC). In the first approach, a priori information about the fault that can affect the system is required. This fault is considered as uncertainties or disturbance which are taken into account in the design of the control law [18]. In contrast, the second approach has the ability to compensate all possible fault on-line. It has the possibility to change structure or to reconfigure the drive according to the information provided by the fault detection block [18].

In this paper, we propose a fault detection and tolerance model which can be seen as an active fault tolerant control model applied to a direct torque control induction motor drive affected by a stator inter turn fault.

The main contributions of this paper are:

1. A new model-based detection technique for DTC induction motor drives under stator inter turn fault.
2. A new fault indicator for stator inter turn fault detection based on state and fault parameters of the machine.

3. An improvement of the DTC drive performance by updating the parameter of the drive (i.e. the stator resistance).

This paper is organized as follows. In Section II, the architecture of a DTC induction motor drive is introduced including the structure of the DTC drive, and the mathematical model of an induction motor under faulty mode is shown. In Section III, the impact of the stator inter turn fault on the behaviour of the DTC drive is introduced. In section IV, Based on this behaviour, a fault detection module is synthesized and a fault tolerant control is designed to reconfigure the DTC drive. The extended Kalman filter (EKF) is chosen as the state and parameter estimation technique for the proposed fault detection and tolerance model. In Section V, the simulation results are shown. Finally, a conclusion closes this paper.

2 DTC induction motor drives

The DTC induction motor drive is gaining ample of interest among the researchers because of its simplicity and fast dynamical response to the change in the operating conditions. The scheme involves minimum computations and requires less PI controllers in comparison to the other control schemes of IM drive's operation. Moreover, DTC-based drives can be tuned with comfort and implemented with ease. Fig. 1 shows a representative block diagram of the DTC scheme for IM drive used for the present investigation of fault detection, and compensation.

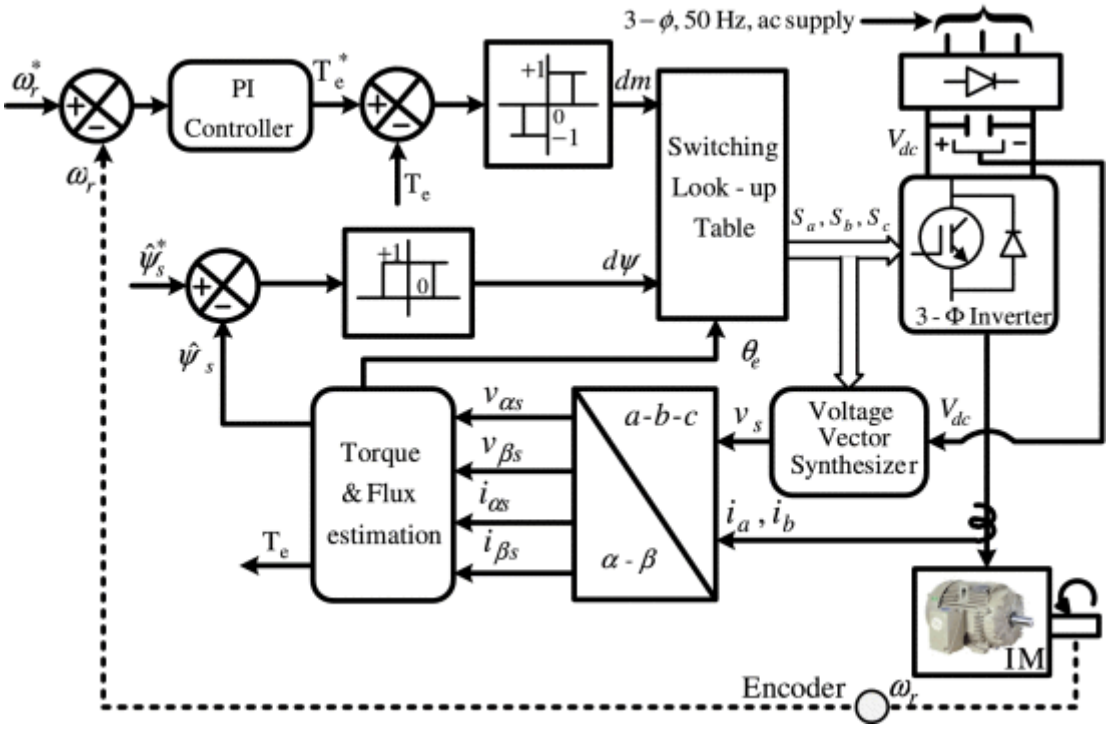

Fig. 1. Structure of a DTC induction motor drive with speed sensor.

2.1 Structure of a DTC drive

The control system of a DTC induction motor drive basically comprises a two-level hysteresis controller, for flux control, and a three-level hysteresis controller for torque

control. These controllers, in conjunction with a switching table, generate the output signals to the gates of the power switches of the inverter (Fig. 1). The role of the flux controller is to maintain the flux level within a narrow hysteresis band around the reference value. On the other hand, the torque controller receives the information obtained from the torque estimator and compares this value with a reference value that can be specified by the user or be the output of a speed controller (in a system with a speed loop). Two current sensors measure the motor supply currents while a voltage sensor measures the dc-link voltage that, in conjunction with the knowledge of the switching status of the six controlled power switches of the inverter, is used to compute the stator voltages of the motor.

The stator flux linkage components, in dq axes, are usually estimated by the equations:

$$\psi_{ds} = \int (v_{ds} - R_s)dt \tag{1}$$

$$\psi_{qs} = \int (v_{qs} - R_s)dt \tag{2}$$

Where R_s is the stator resistance and subscripts ds and qs stand for the d-axis and q-axis components of the voltages and currents of the stator windings of the motor.

The electromagnetic torque developed by the motor is estimated by

$$\widehat{T_e} = \frac{3}{4}\mathrm{P}(\psi_{ds} i_{ds} - \psi_{qs} i_{qs}) \tag{3}$$

Where P is the number of poles.

2.2 qd MODEL OF AN INDUCTION MACHINE UNDER STATOR WINDING INTER-TURN SHORT CIRCUIT FAULT

2.2.1 Description of Stator Winding Inter-Turn Short Circuit Fault and Fault Parameters

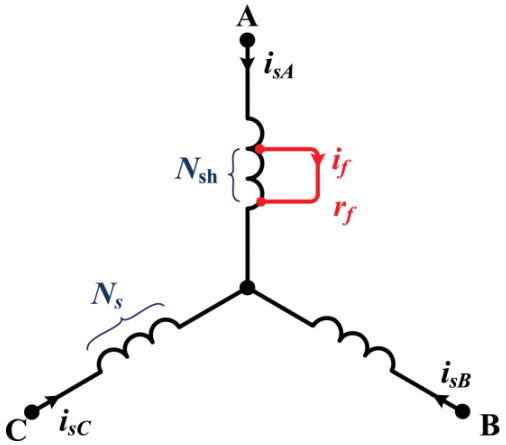

Fig. 2. Stator winding under inter-turn short circuit fault in phase a.

Fig. 2 shows the stator winding of a star-connected three phase induction machine under inter-turn fault in phase a. The fault is represented by the fraction of shorted turn μ,

the fault loop current i_f and the fault loop resistance r_f. The fraction of shorted is described as:

$$\mu = \frac{N_{sh}}{N_s} \tag{4}$$

2.2.2 IM Faulty model

In order to design and evaluate the diagnosis strategies, a motor model that allows the inclusion of the fault effects is needed. A dynamic IM model including inter-turn short circuits in the phase a winding, as shown in Fig. 2 is proposed in [19]. The set of equations, adopted from [19] describing the faulty machine is as follows:

$$v_{qds} = R_s i_{qds} + \frac{d\psi_{qds}}{dt} - \mu R_s i_f \begin{bmatrix} \frac{2}{3} & 0 \end{bmatrix}^T \tag{5}$$

$$0 = R_r i_{qdr} + \frac{d\psi_{qdr}}{dt} - \omega_r \begin{bmatrix} 0 & -1 \\ 1 & 0 \end{bmatrix} \psi_{qdr} \tag{6}$$

$$\psi_{qds} = L_s i_{qds} + L_m i_{qdr} - \mu L_s i_f \begin{bmatrix} \frac{2}{3} & 0 \end{bmatrix}^T \tag{7}$$

$$\psi_{qdr} = L_r i_{qdr} + L_m i_{qds} - \mu L_m i_f \begin{bmatrix} \frac{2}{3} & 0 \end{bmatrix}^T \tag{8}$$

$$r_f i_f = \mu R_s (i_{qs} - i_f) + \frac{d\psi_f}{dt} \tag{9}$$

$$\psi_f = \mu (L_s i_{qs} - L_m i_{qr}) - \mu i_f (L_{ls} + \frac{2}{3} \mu L_m) \tag{10}$$

$$T_e = \frac{3P}{4} L_m (i_{qs} i_{dr} - i_{ds} i_{qr}) - \frac{P}{2} \mu L_m i_f i_{dr} \tag{11}$$

$$\frac{d\omega_r}{dt} = \frac{P}{2} (T_e - T_l - B\omega_r) \tag{12}$$

$$L_f \frac{di_f}{dt} = -R_f i_f + \mu v_{qs} \tag{13}$$

$$L_f = \mu (1 - \frac{2}{3} \mu) L_{ls} \tag{14}$$

$$R_f = \mu \left(1 - \frac{2}{3} \mu\right) R_s + r_f \tag{15}$$

In the equations above, v_{qds} = $[\, v_{qs} \quad v_{ds}]^T$, i_{qds} = $[\, i_{qs} \quad i_{ds}]^T$, ψ_{qds} =$[\, \psi_{qs} \quad \psi_{ds}]^T$, ψ_{qdr} =$[\, \psi_{qr} \quad \psi_{dr}]^T$, v_{qds} =$[\, v_{qs} \quad v_{ds}]^T$. v_{qs}, v_{ds} are the q-axis and d-axis components of stator voltage. ψ_{qs}, ψ_{ds} are the q-axis and d-axis components of stator flux linkages. ψ_{qr}, ψ_{dr} are the q-axis and d-axis components of rotor flux linkages. i_{qs}, i_{ds} are the q-axis and d-axis components of stator current. i_{qr}, i_{dr} are the q-axis and d-axis components of rotor current. ψ_f is the flux linkage of the faulty winding portion. i_f is the fault loop current, r_f is the insulation resistance of the fault loop current, L_f is the magnetizing inductance of the faulty winding portion, T_e is the electromagnetic torque. ω_r is the rotor speed. R_s, R_r are

the stator resistance and rotor resistance, respectively. L_s, L_{ls}, L_r, L_m are the stator inductance, stator leakage inductance, rotor inductance, and magnetizing inductance, respectively. P is the number of poles. T_l is the load torque and B is the friction coefficient.

3 Impact of inter turn fault on the behaviour of the DTC drive

The impact of inter turn fault have been studied by the authors [20] and [21]. This paper show a brief description of these studies for the purpose to develop the fault detection and tolerance model. For more details refer to these references.

3.1 Problem of the torque estimation

When there is no fault (μ = 0), the estimated electromagnetic torque is the true value:

$$\widehat{T_e} = \frac{3P}{4}(\psi_{ds} i_{ds} - \psi_{qs} i_{qs}) \tag{3}$$

However, on the fault onset, if the degree of fault is small and the short circuit is not bold (r_f>0), the DTC continues its apparent normal operation. In this situation the estimated electromagnetic torque can only be evaluated as the IM is healthy and no information is provided about the faulty quantities. In this situation the torque estimation would be erroneous and it will differ from the actual value. The only correct information gathered by the DTC is the stator currents and voltages, however, it has been proven and found in literature that the controller keeps its normal operation under certain range of severity fault.

The electromagnetic torque developed by the motor with an inter-turn short circuit in winding is given by:

$$T_e = \frac{3P}{4} L_m(i_{qs} i_{dr} - i_{ds} i_{qr}) - \frac{P}{2} \mu L_m i_f i_{dr} \tag{11}$$

Equation (11) can be rewritten as given in [20] by:

$$T_e = (\frac{3P}{4}(\psi_{ds} i_{ds} - \psi_{qs} i_{qs})) + (\frac{P}{2} \mu L_m i_f i_{qr} + \frac{P}{2} \mu L_m i_f i_{qs} \underbrace{(L_m + \mu L_{ls})}_{\cong L_m}) \tag{16}$$

The first term of (16) is the one characteristic of a healthy motor. When the motor has no faults, (11) and (16) are equivalent. In this case, the torque estimator of the drive gives an accurate estimation of the “true” value of the electromagnetic torque developed by the motor. On the other hand, when short circuits arise, the first term of (16) is the only one that can be evaluated by the torque estimator of the drive because no information is provided about the quantities present in the other terms. Hence, the error arising from the wrong estimation of the electromagnetic torque is given by:

$$T_{error} = \frac{P}{2} \mu L_m i_f (i_{qs} + i_{qr}) \tag{17}$$

Reference [20] demonstrates that, neglecting the high order space harmonics in a line-connected motor under the presence of stator inter-turn short circuits, the currents involved in (17) can be expressed as:

$$i_f(t) = I_f \cos(\omega t + \beta_1) \tag{18}$$

$$i_{qs}(t) + i_{qr}(t) = \mathrm{A}\cos(\omega t + \beta_2) \tag{19}$$

Where ω is the angular supply frequency, I_f is the amplitude of the short circuit current and A is a constant. Hence, considering (17), (18), and (19), the torque error will be given by:

$$T_{error}(t) = \underbrace{B}_{static\ eror} + \underbrace{\mathrm{Ccos}(\,2\omega t + \beta_3)}_{T_{dyn}=dynamic\ error} \tag{20}$$

Where B and C do not depend on the variable time. This equation clearly demonstrates that under the presence of the fault, there is a static error, which is constant, and a dynamic error that corresponds to an oscillating torque component at the double supply frequency.

3.2 Reaction to the control system

Let us assume that the motor is running smoothly, with a constant load. When the stator fault arises, its first effects are the appearance of a negative-sequence component, and the introduction of an additional quantity in the positive-sequence component of the motor supply currents. According to this, the space phasor of the stator currents can be expressed as:

$$\underline{i_s(t)} = I_s^+ e^{(j\omega t+\alpha)} + I_s^- e^{(j\omega t+\phi)} \tag{21}$$

Where $I_s^+$and I_s^- stand for the amplitude of the positive and negative sequence components of the stator currents, respectively. Neglecting the stator resistance, the flux controller has no reason to react to this new condition, at least for now, and will continue to impose a sinusoidal flux at the fundamental supply frequency. Thus, before the reaction of the control system to the presence of the fault, the space phasor of the stator flux linkage can be given by:

$$\underline{\psi_s(t)} = \psi_{ref} e^{(j\omega t)} \tag{22}$$

Where ψ_{ref} is reference flux of the DTC drive. The torque, as estimated by the control system, is given by (3) or equivalently by:

$$\widehat{T_e} = \frac{3P}{4} Im\left\{\underline{\psi_s^*}\underline{i_s}\right\} \tag{23}$$

Taking into account (21)–(23), the estimated torque is equal to:

$$\widehat{T_e} = \frac{3P}{4}\psi_{ref} I_s^+ \sin(\alpha) - \underbrace{\frac{3P}{4}\psi_{ref} I_s^- \sin(2\omega t + \phi)}_{T1} \tag{24}$$

The previous expression shows that the torque, as calculated by the control system, contains a constant term and an alternating component T_1 at twice the fundamental supply frequency.

On the other hand, it is known that the torque controller forces the estimated torque to lie within a narrow hysteresis band around a reference value. This means that the estimated torque has to follow the reference value, no matter the condition of the motor, and the controllers have to cancel a torque component with a frequency of $2f$ and an amplitude of $\frac{3P}{4}\psi_{ref} I_s^-$ which mean that the control system has to introduce a torque component equal to:

T_{ad}=-T_1.

By the analysis of (23), it is possible to conclude that there are two immediate possibilities to achieve this:

1. The introduction of a negative-sequence component in the stator flux (and, consequently, in the motor supply voltages), which will try to compensate the motor asymmetry and
2. The introduction of a positive-sequence component in the stator flux linkage, at a frequency of $3f_s$. The interaction of each one of these components with the positive-sequence component of the supply currents at the frequency f_s may produce a component in the electromagnetic torque at a frequency of $2f_s$ with a phase opposite to that of the torque component which it is intended to cancel.

It is concluded that there is not too much room for introducing a negative sequence voltage, as this is limited by the flux narrow hysteresis band. The second possibility (preferred by the authors of [20]) is the introduction of third harmonic component in the flux and by consequence in the stator currents and voltages by the torque hysteresis controller to compensate the double frequency torque component.

3.3 Amplification of the torque oscillations

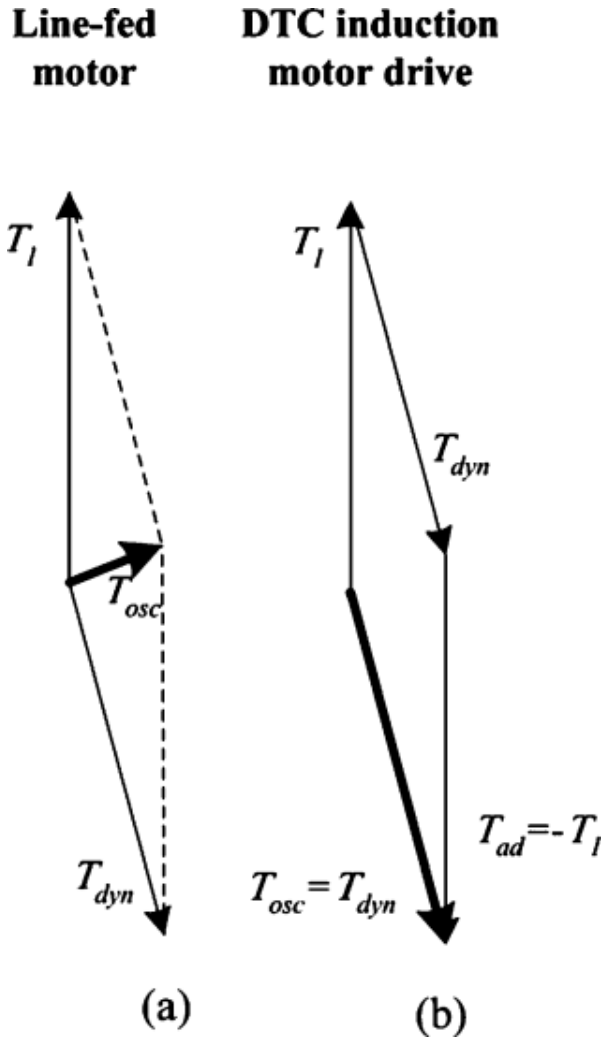

Fig. 3. Illustration of the process of amplification of the torque oscillations caused by the control system of a DTC induction motor drive with a stator fault.

Another interesting aspect related to the behaviour of this type of drive in the presence of stator faults explained by the authors of [20] is that, although the reference torque is constant and the action of the controllers of the drive force the estimated torque to lie within the limits of the torque hysteresis band around the reference value, the inspection of (17) and (3) shows that the "true" torque developed by the motor is equal to the reference value, plus the torque error given by (17). Two reasons contribute for making this torque error quite significant: the fact that the short-circuit current is usually very high and the fact that, although for a symmetrical machine the sum of the current components is usually small, when the machine develops stator faults this sum will contain an appreciable alternating component, with special emphasis on the component at the fundamental supply frequency. Consequently, the predominant components of the torque actually developed by the motor are the dc component, imposed by the load of the motor, and the alternating component at the double supply frequency. This alternating component reinforces the one that would exist based solely on the effects of the stator fault. This aspect can be easily explained with the aid of a graphical illustration (Fig. 5). Let us consider a motor directly connected to the grid, with a given stator fault. In these conditions, the "true" torque developed by the motor is equal to:

$$T_e = \frac{3P}{4}(\psi_{ds} i_{ds} - \psi_{qs} i_{qs}) + \frac{P}{2}\,\mu L_m i_f (i_{qs} + i_{qr}) \tag{25}$$

This torque has a constant term and an oscillating component at a frequency of $2f_s$. This last component is equal to the sum of two oscillating components, originated by the two terms of the second member of (18). Thus, the total oscillating torque component is equal to:

$$T_{osc} = T_1 + T_{dyn} \tag{26}$$

Where T_1 and T_{dyn} were previously defined in (21) and (17), respectively. Hence, if this motor is connected to the grid, it will exhibit a total torque oscillation as illustrated in Fig. 5(a).

When the motor is part of a DTC drive, running at the same load level and with the same fault, the torque controller will introduce an additional torque component T_{ad}=−T_1. From the torque controller point of view, the motor is operating with no torque oscillations as:

$$T_{osc} = T_1 + T_{ad} = T_1 - T_1 = 0 \tag{27}$$

But in reality the motor is operating with an oscillating torque component given by:

$$T_{osc} = T_1 + T_{ad} + T_{dyn} = T_1 - T_1 + T_{dyn} = T_{dyn} \tag{28}$$

This fact is illustrated in Fig. 5(b). Comparing T_{osc} in Fig. 5(a) and (b), it is evident that the torque oscillations are much higher in the case of the DTC drive. In this case, the drive will operate with a constant torque error, which may not be noticed if the drive is operating with a speed loop because in this case the output of the speed controller will correct the reference value given to the torque controller, and with a significant oscillating torque component at the double supply frequency, much higher than the one that would exist if the motor was directly connected to the grid. In this sense, it can be stated that the control system of the DTC drive acts as an amplifier of the torque oscillations primarily caused by the stator fault. This may be a potential problem when the DTC drive runs without a speed loop

(torque reference mode), besides the additional mechanical stresses imposed to the shaft of the motor.

In conclusion it has been found that the first reaction of the DTC controller to the inter turn fault is the increase in the 3rd order harmonic component of, to counter balance the oscillatory component in the developed torque. That's the reason why in [20] Motor Current Signature Analysis (MCSA) was used and the 3rd order harmonic component was adopted for fault diagnosis. As the inter turn fault will introduce a 2nd order harmonic component in the developed torque, the developed power will inherit the same signature. Consequently in [22], the fault detection was based on monitoring of the 2nd order harmonic component of the developed power, for DOL connected IM and DTC driven IM. The fault diagnosis or inter turn faults in DTC driven IMs based on the off-diagonal components of the symmetrical components impedance matrix was presented in [23]. Finally, the fault diagnosis of inter turn faults in DTC driven IMs based on mathematical morphological gradient was presented in [24].

From the aforementioned literature survey, it is obvious that researches have investigated fault diagnosis of inter turn faults in DTC driven IMs by monitoring the 3rd order harmonic in the stator current and the 2nd order harmonic in the developed torque either in frequency domain, or in time domain. None of the aforementioned researches dealt with the estimation of the quantities which produce the torque oscillations T_{dyn} due to the inter turn fault.

The contribution of this study to the current state-of-the-art is the development of a fault detection technique and fault tolerant control based on state and parameter identification strategies for DTC induction motor drives. The fault detection and tolerance technique is able to detect inter turn fault at the incipient stage and improve the DTC performance under inter turn fault, as shown in the next section.

4 Proposed fault detection and tolerance model

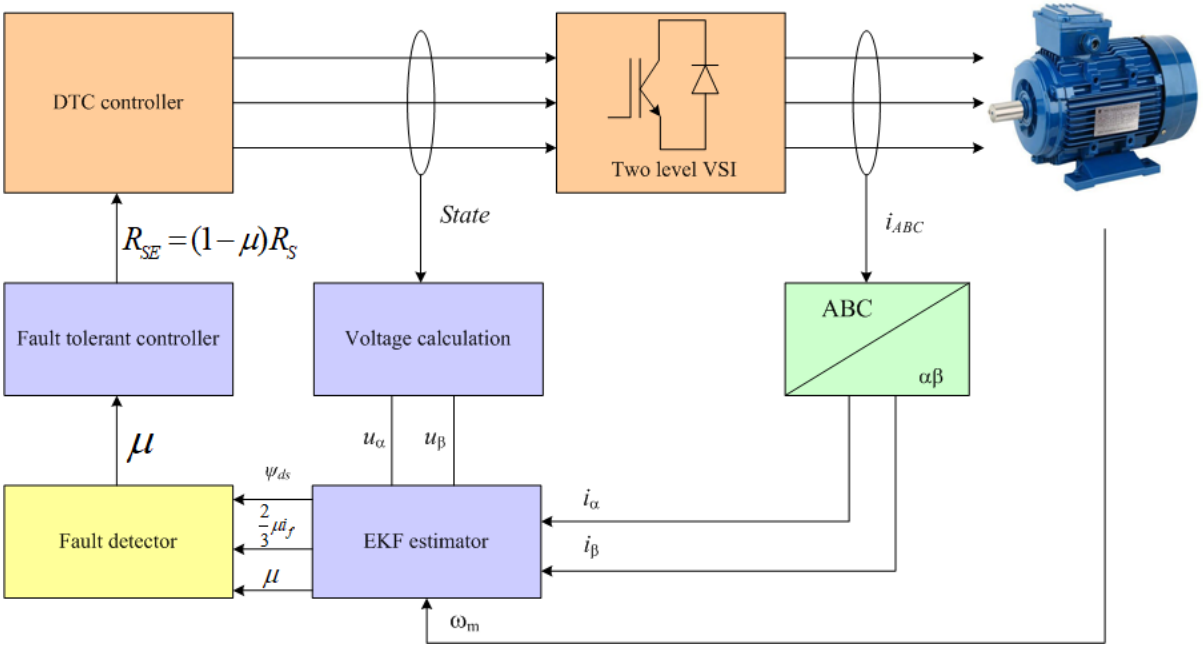

Fig. 4. Block diagram of the proposed model-based fault detection tolerant technique for DTC induction motor drives under stator inter turn fault.

Fig.4. shows the main idea underlying the development of the detection technique and fault tolerant control presented in this paper. First by estimating the state and fault parameters of the motor, we can reconstruct the oscillation that would appear in the developed torque if the DTC induction drive is under a stator inter turn. A fault indicator is then calculated based on these estimations. Once the fault is detected, the fault tolerant control block reconfigures the DTC drive by updating one of these parameters. This parameter is the stator resistance, tuned using the fault severity factor estimated by the designed estimator.

4.1 New inter-turn fault indicator calculation

The error arising from the wrong estimation of the electromagnetic torque is given by:

$$T_{error} = \frac{P}{2}\,\mu L_m i_f (i_{qs} + i_{qr}) \tag{17}$$

Let's try to rewrite this expression by a further mathematical manipulations. The expressions of the stator flux linkages under inter turn fault are:

$$\psi_{qs} = L_s i_{qs} + L_m i_{qr} - \frac{2}{3}\mu L_s i_f \tag{29}$$

$$\psi_{ds} = L_s i_{ds} + L_m i_{dr} \tag{30}$$

From these equations we get these two equations:

$$L_m i_{qr} = \psi_{qs} - L_s i_{qs} + \frac{2}{3}\mu L_s i_f \tag{31}$$

$$L_m i_{dr} = \psi_{ds} - L_s i_{ds} \tag{32}$$

The developed torque under inter turn fault is:

$$T_e = \frac{3P}{4}\,L_m (i_{qs} i_{dr} - i_{ds} i_{qr}) - \frac{P}{2}\,\mu L_m i_f i_{dr} \tag{11}$$

By replacing (31) and (32) in (11), we get a new expression of the developed torque:

$$T_e = \frac{3P}{4}(\psi_{ds} i_{ds} - \psi_{qs} i_{qs}) - \frac{P}{2}\,\mu i_f \psi_{ds} \tag{33}$$

The electromagnetic torque estimated by the DTC drive is:

$$\widehat{T_e} = \frac{3P}{4}(\psi_{ds} i_{ds} - \psi_{qs} i_{qs}) \tag{3}$$

Hence, the new expression of the error arising from the wrong estimation of the electromagnetic torque is given by:

$$T_{error} = \widehat{T_e} - T_e = \frac{P}{2}\,\mu i_f \psi_{ds} \tag{34}$$

This expression depends on the d-axis stator flux, fault severity factor and fault loop current.

By rewriting as function of the d-axis stator flux and the complete fault signal $\frac{2}{3}\,\mu i_f$, this expression becomes:

$$T_{error} = \frac{3P}{4}\frac{2}{3}\mu i_f \psi_{ds} \quad (35)$$

This expression is easy to estimate by choosing a proper estimator.

Its normalized modulus is used in this paper as a severity factor:

$$Severity_{factor} = \frac{\left|\frac{3P}{4}\frac{2}{3}\mu i_f \psi_{ds}\right|}{\sqrt{2} I_{nom} \psi_{ref}} \quad (36)$$

Where I_{nom} is the nameplate rms value of the motor current, and ψ_{ref} the reference flux.

As it can be seen, the new fault indicator is proportional to the fault current and the number of short circuited turns, which makes it a reliable fault detector. By using this component for fault detection, it is possible to detect incipient faults, either due to the increase of the fault current or the number of short-circuited turns. The use of this fault detector also allows us to avoid false alarms due to parameter errors or load and speed variations.

4.2 Fault compensation method

The resistance of a coil is directly proportional to the number of turns in the coil, hence the resistance of the short-circuited stator and the un-short circuited part of phase a are given by:

$$r_f = \mu R_s \quad (37)$$

$$R_{s\_unshorted} = (1-\mu) R_s \quad (38)$$

Equation (38) shows that stator winding turn fault causes reduction in the turns of winding resistance by μ%.

When there is no fault (μ = 0), the estimated stator flux-linkage is given by:

$$\psi_{ds} = \int (v_{ds} - R_s) dt \quad (1)$$

$$\psi_{qs} = \int (v_{qs} - R_s) dt \quad (2)$$

In the presence of inter turn fault, the DTC continues its apparent normal operation. In this situation, the estimated flux-linkage can only be evaluated with (1) and (2) using R_s. However the true value of the stator resistance inside the motor is given by:

$$R_{s\_unshorted} = (1-\mu) R_s \quad (38)$$

As the estimation of the stator flux depends on stator resistance, a wrong value of this stator resistance will affect the performance of the DTC drive, leading to a wrong estimation of stator flux and consequently of the electromagnetic torque and the stator flux position.

The fault tolerant control is obtained by estimating the fault severity factor and then, when the fault is detected by the fault detection block, the true value of the stator resistance is estimated using the equation

$$R_{s\_unshorted} = (1-\mu) R_s \quad (38)$$

This value is fed to the DTC drive to update the parameter of it control algorithm. A similar method to improve the performance of the DTC drive was used in [25]. But instead of to

estimate the fault severity factor using an estimator, the authors used an artificial neural network.

4.3 Extended Kalman Filter as estimator for state and parameter identification

In order to design the model, some quantities must be estimated using an estimator. This paper proposes to use the stator quantity and stator winding fault parameters for the development of the fault detection and tolerance model of the DTC induction motor drive. The focused stator quantity is the d-axis stator flux linkage current ψ_{ds} . The fault parameters of interest are the complete fault signal $\frac{2}{3}\mu i_f$ (product of the fault severity factor μ, and the fault loop current $\frac{2}{3}i_f$) and the fault severity factor μ.

The state and parameter estimation is a key subsystem of the proposed model.

4.3.1 EKF algorithm

The EKF is a mathematical tool which allows to determinate the unmeasurable states and parameters by using measurable physical quantities. It is one of the widely used state/parameter estimation techniques in industrial applications. The EKF is a recursive optimum state estimator for nonlinear systems. It is robust to model inaccuracy, parameter variations, and measurement noise [26].

Consider the following general expression of a nonlinear system:

$$\begin{cases} \dot{X}(t) = f\big(X(t), \lambda(t), U(t)\big) + W(t) \\ Y(t) = h\big(X(t), \lambda(t), U(t)\big) + V(t) \end{cases} \quad (39)$$

Where f and h correspond to the state and output equations of the nonlinear model, respectively. $W(t)$ and $V(t)$ are the state and measurement noises vectors with covariance matrices Q and R, respectively.

In order to estimate one or several parameters λ in the model, additional state variables are added to (39), resulting in the following extended nonlinear system:

$$\begin{cases} \dot{X}_e(t) = \begin{bmatrix} \dot{X}(t) \\ \dot{\lambda}(t) \end{bmatrix} = \begin{bmatrix} f\big(X_e(t), U(t)\big) \\ 0 \end{bmatrix} + \begin{bmatrix} W_X(t) \\ W_\lambda(t) \end{bmatrix} \\ Y(t) = h_e\big(X_e(t), U(t)\big) + V(t) \end{cases} \quad (40)$$

Where X_e is the extended state vector. The additional equation $\dot{\lambda}(t)$= $W_\lambda(t)$ reflects that the dynamic response of the estimated parameters is assumed unknown.

For the EKF algorithm application, this nonlinear model must be discretized and linearized around the current state (using Jacobian matrices).

The steps of the estimation procedure of an extended Kalman filter are given by:

- The prediction of the extended state vector:

$$\dot{X}(k+1/k) = f\left(\dot{X}(k/k), u(k)\right) \quad (41)$$

- The prediction of the covariance matrix:

$$P(k+1/k) = A(k)\, P(k/k) A^T(k) + Q \quad (42)$$

Where:

$$A(k) = \frac{\partial f}{\partial x}(x(k)u(k)\Big|_{x = \dot{x}(k/k)}$$

- Computation of Kalman gain:

$$K(k+1) = P(k+1/k)C^T(k)((C(k)P(k+1/k)C^T(k) + R)\,)^{-1} \quad (43)$$

- State update:

$$\dot{X}(k+1/k+1) = \dot{X}(k+1/k) + K(k+1)[y(k+1) - C(\dot{X}(k+1/k))] \quad (44)$$

- Estimation covariance computation:

$$P(k+1/k) = \big(I - K(k+1)C(k)\big)P(k+1/K) \quad (45)$$

4.3.2 State-space model of a faulty induction motor

The state-space model of a faulty model can be derived from its qd model.

Let's define $x_1 = i_{ds}$, $x_2 = i_{qs}$, $x_3 = \psi_{ds}$, $x_4 = \psi_{qs}$, $x_5 = \frac{2}{3}\mu i_f$ and the state vector

$x = [x_1\ x_2\ x_3\ x_4\ x_5]^T$, then the state equations are:

$$\begin{cases} \dfrac{dx}{dt} = A(\omega_r)x + Bu \\ y = Cx \end{cases} \quad (46)$$

Where:

$$A(\omega_r) = \begin{bmatrix} -a & -\omega_r & b & c\omega_r & \omega_r \\ \omega_r & -a & c\omega_r & b & \left(a - \dfrac{R_f}{L_f}\right) \\ & & & 0 & 0 \\ -R_s & 0 & 0 & 0 & R_s \\ 0 & -R_s & 0 & & \\ 0 & 0 & 0 & 0 & -\dfrac{R_f}{L_f} \end{bmatrix} \quad (47)$$

$$B = \begin{bmatrix} c & 0 \\ & (c + \dfrac{2}{3}\dfrac{\mu^2}{L_f}) \\ 0 & \\ 1 & 0 \\ 0 & 1 \\ 0 & \dfrac{2\mu^2}{3L_f} \end{bmatrix} \quad (48)$$

$$u = \begin{bmatrix} v_{ds} \\ v_{qs} \end{bmatrix} \quad (49)$$

$$C = \begin{bmatrix} 1 & 0 & 0 & 0 & 0 \\ 0 & 1 & 0 & 0 & 0 \end{bmatrix} \quad (50)$$

$$a = \left(\frac{R_s}{L_\sigma} + \frac{R_r L_s}{L_r L_\sigma}\right) \quad (51)$$

$$b = \frac{R_r}{L_r L_\sigma} \quad (52)$$

$$c = \frac{1}{L_\sigma} \quad (53)$$

$$L_\sigma = L_s \sigma \quad (54)$$

$$\sigma = \frac{L_s L_r - {L_m}^2}{L_s L_r} \quad (55)$$

In order to estimate fault parameter μ, a system augmentation technique can be utilized by considering this parameter as additional state variable. The resultant system becomes six-order system.

This system is more complex to estimate the states ψ_{ds}, $\frac{2}{3}\mu i_f$ and the parameter μ. Therefore to simplify the model, if defining new state variable:

$$x_6 = \frac{\mu}{1 - \frac{2}{3}\mu} \quad (56)$$

We can use an equality constraint on fault parameter define by [27]:

$$k_f = \frac{r_f}{\mu^2} \quad (57)$$

Where:

$$k_f = \left|\frac{\widetilde{V_{sp}}}{\Delta_n}\right| \quad (58)$$

$$\Delta_n = \widetilde{I_{sn}} - \frac{\widetilde{V_{sn}}}{Z_n} \quad (59)$$

$$Z_n = (R_s + j\omega_s L_s) + \frac{\omega_s^2 L_m^2}{\frac{R_r}{(2-s)} + j\omega_s L_r} \quad (60)$$

Where V_{sp}, V_{sn} are positive and negative components of stator voltage, I_{sn} is negative components of stator current, ω_s is electrical frequency, and s is motor slip.

The estimation of μ is deduced from (56) by:

$$\mu = \frac{x_6}{1 + \frac{2}{3}x_6} \quad (61)$$

The terms $\frac{R_f}{L_f}$ and $\frac{2\mu^2}{3L_f}$ in matrices A and B can be expressed as:

$$\frac{R_f}{L_f} = \frac{R_s}{L_{ls}} + \frac{k_f}{L_{ls}} x_6 \quad (62)$$

$$\frac{2\mu^2}{3L_f} = \frac{2}{3L_{ls}} x_6 \tag{63}$$

With:

$$L_f = \mu(1 - \frac{2}{3}\mu)L_{ls} \tag{14}$$

$$R_f = \mu\left(1 - \frac{2}{3}\mu\right)R_s + r_f \tag{15}$$

The new state vector becomes:

$$x_n = [x^T \quad x_6]^T \tag{64}$$

Its associated state equations are:

$$A_n(\omega_r, v_{qs}) = \begin{bmatrix} -a & -\omega_r & b & c\omega_r & \omega_r & 0 \\ \omega_r & -a & -c\omega_r & b & (a - \frac{R_s}{L_{ls}} + \frac{k_f}{L_{ls}} x_6) & \frac{2}{3L_{ls}} v_{qs} \\ -R_s & 0 & 0 & 0 & 0 & 0 \\ 0 & -R_s & 0 & 0 & R_s & 0 \\ 0 & 0 & 0 & 0 & -(\frac{R_s}{L_{ls}} + \frac{k_f}{L_{ls}} x_6) & \frac{2}{3L_{ls}} v_{qs} \\ 0 & 0 & 0 & 0 & 0 & 0 \end{bmatrix} \tag{65}$$

$$B_n = \begin{bmatrix} c & 0 \\ 1 & c \\ 0 & 0 \\ 0 & 1 \\ 0 & 0 \\ 0 & 0 \end{bmatrix} \tag{66}$$

$$u = \begin{bmatrix} v_{ds} \\ v_{qs} \end{bmatrix} \tag{67}$$

$$C = \begin{bmatrix} 1 & 0 & 0 & 0 & 0 & 0 \\ 0 & 1 & 0 & 0 & 0 & 0 \end{bmatrix} \tag{68}$$

4.3.3 The choice of the covariance matrix Q and R

It is through these matrixes that pass the different states measured, predicted and estimated. Their main is to minimize the errors related to the modelling approximation and the presence of noise on the measurements. The matrix Q, related to noise content in the state, adjusts the quality of our estimated model and its sampling. A greater value of Q gives a higher value of gain "K", reducing the importance of the modelling and dynamic of the filter. The measure has then a relative weight greater. A high value of Q can create however the instability of the estimator. The matrix R adjusts the weight measurements. A high value indicates a large uncertainty of the measure. A low value gives significant weight to the measure. However, it's being careful for the risk of instability at low values of R.

Covariance matrixes are selected by trial-and-errors for achieving a desired estimation performance, as below:

$$\mathrm{Q} = \mathrm{diag}\,[7.10^{-6} \quad 7.10^{-6} \quad 7.10^{-6} \quad 7.10^{-6} \quad 10^{-10} \quad 10^{-10}] \tag{69}$$

$$R = \text{diag}\,[10^{-4} \quad 10^{-4}] \tag{70}$$

4.4 Proposed fault detection and tolerance algorithm for DTC induction motor drives

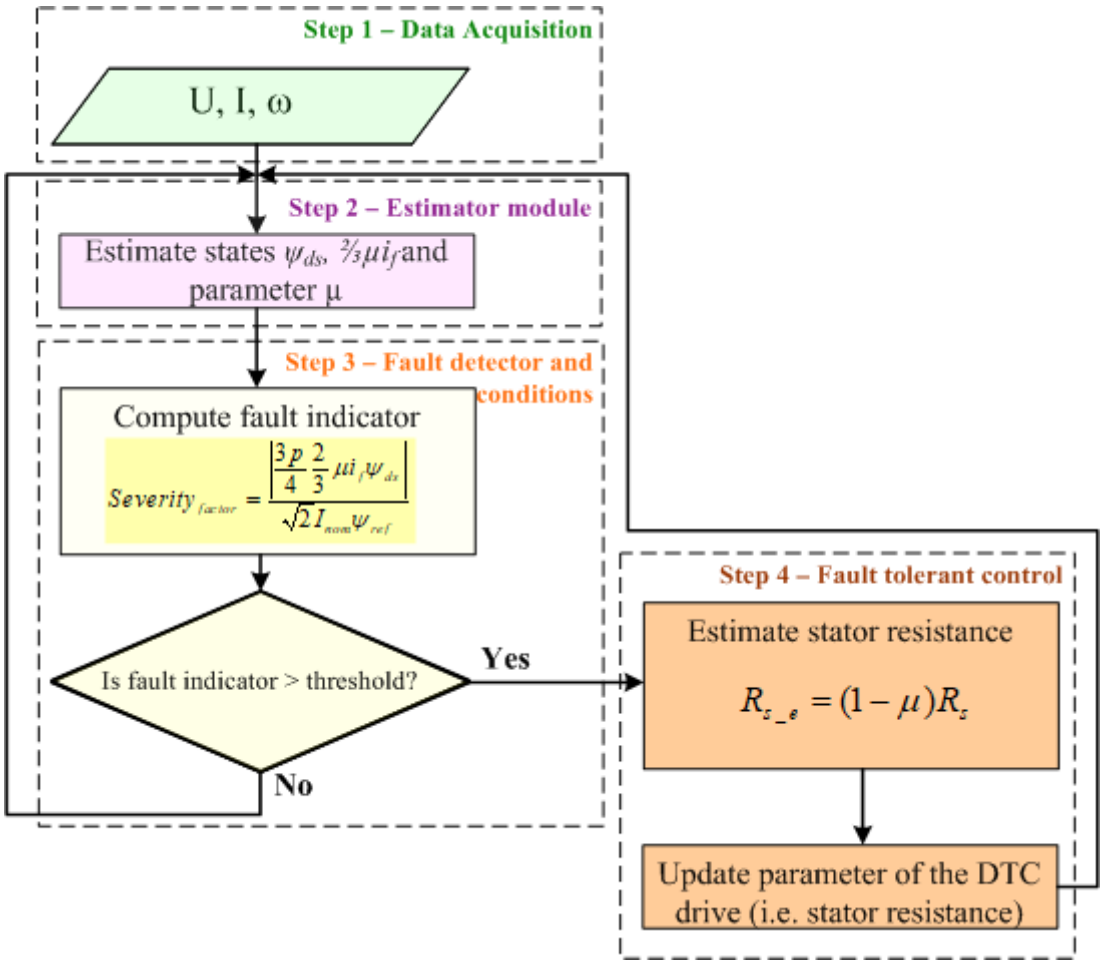

Fig. 5. Proposed model-based fault detection and tolerance algorithm for DTC induction motor drives under stator inter turn fault algorithm.

Fig. 5 shows the flowchart of the proposed fault detection and tolerance algorithm for the DTC induction drive. The proposed algorithm has four steps. The first step acquires the stator currents, stator voltages and mechanical speed. The stator currents are acquired from sensor, while voltages are calculated from the dc voltage and switching states. The speed is acquired from sensor but can be also estimated using an estimator. The second step estimates the states and the parameter used for calculating the fault indicator, using an EKF estimator. In this module, the equality constraint on fault parameters is also calculated using positive and negative components of stator voltage, negative component of stator current and motor slip. The negative and positive components of stator voltage and stator current are determined using the acquired stator currents and voltages. The third step detects the inter turn fault. The severity factor is calculated using the states and parameter estimated in the second step. If its normalized modulus is greater than the threshold value else the fourth step will be executed. The threshold values in the algorithm can be determined in offline

analysis of the magnitude of identified fault signature under various operating conditions such as healthy, various degrees of inter turn fault, and load unbalance. The fourth step of the algorithm estimates the true value of the stator resistance under inter turn fault using the severity factor estimated in the second step. Once the true value of the stator resistance is estimated, this value is fed to the DTC drive to update the parameter of it control algorithm.

5 Simulation results

The technique presented in the previous sections, has been implemented in the MATLAB/Simulink environment. The simulation is conducted for a low-voltage DTC induction motor drive whose parameters are as in Table I.

5.1 DTC induction motor drive simulation

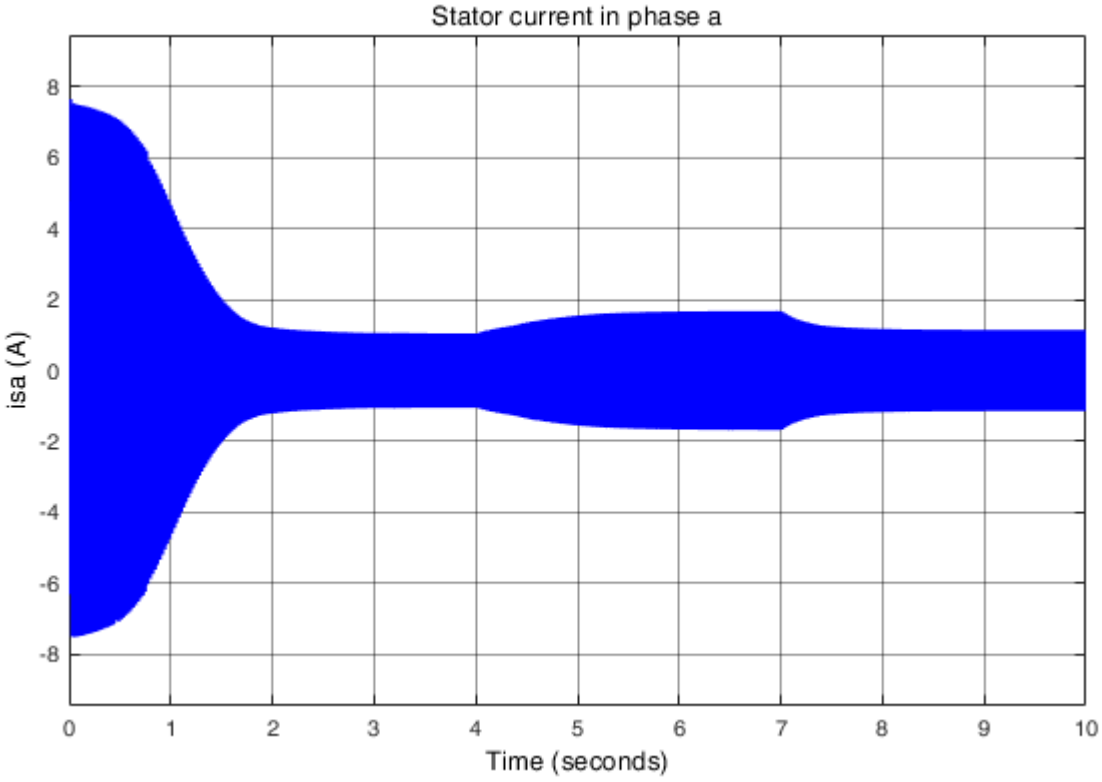

Fig. 6. Simulated stator current in phase a.

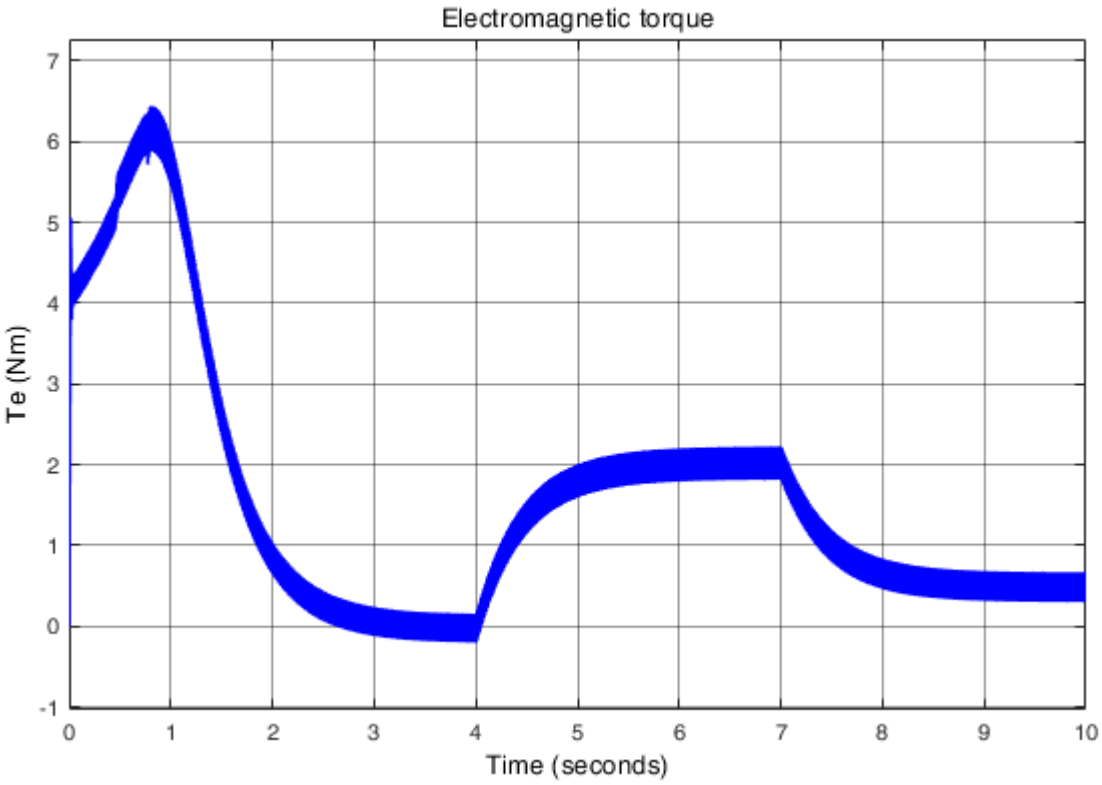

Fig. 7. Developed torque.

The tolerance bands δT and $\delta\lambda$ for the torque and flux comparators are adjusted such that the average switching frequency f_{sw} of the switching devices is around 800 Hz. The stator flux reference ψ_{ref} is set to its rated value of 0.56 Wb.

The entire time for the simulation is 10 sec. The simulation integration step time is 10^{-5}sec. The motor operates at the rated speed under no-load conditions. The start-up is from stand-still until reaching the maximum speed with 300 V_{dc}. The load torque T_l is suddenly increased to its rated value of 2 Nm at t = 4s and then decreased to 0.5 Nm at t = 7s.

Fig. 6 and 7 show the waveforms of the developed torque and the stator current in the phase a, for a healthy DTC induction motor drive. The generated torque T_e responds quickly. The torque ripple is set by the torque tolerance band δT. The stator current i_{as} varies with T_e accordingly.

5.2 The fault detection and tolerance demonstration.

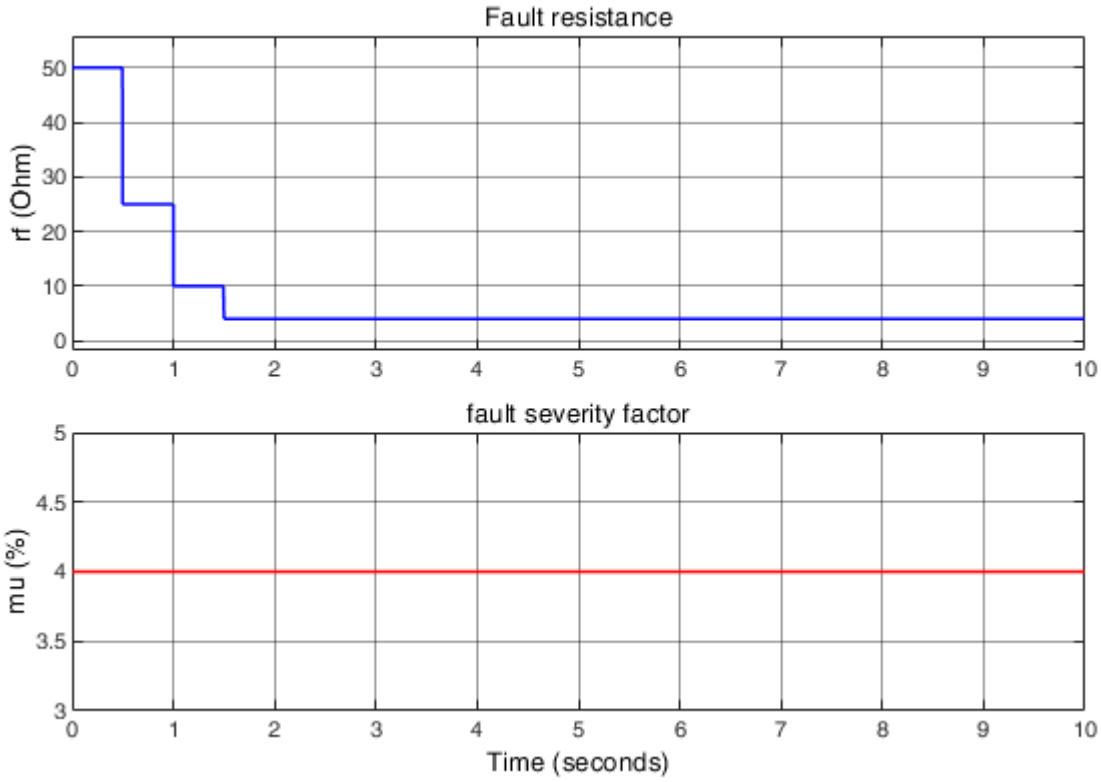

Fig. 8. Fault parameters development for Case 1.

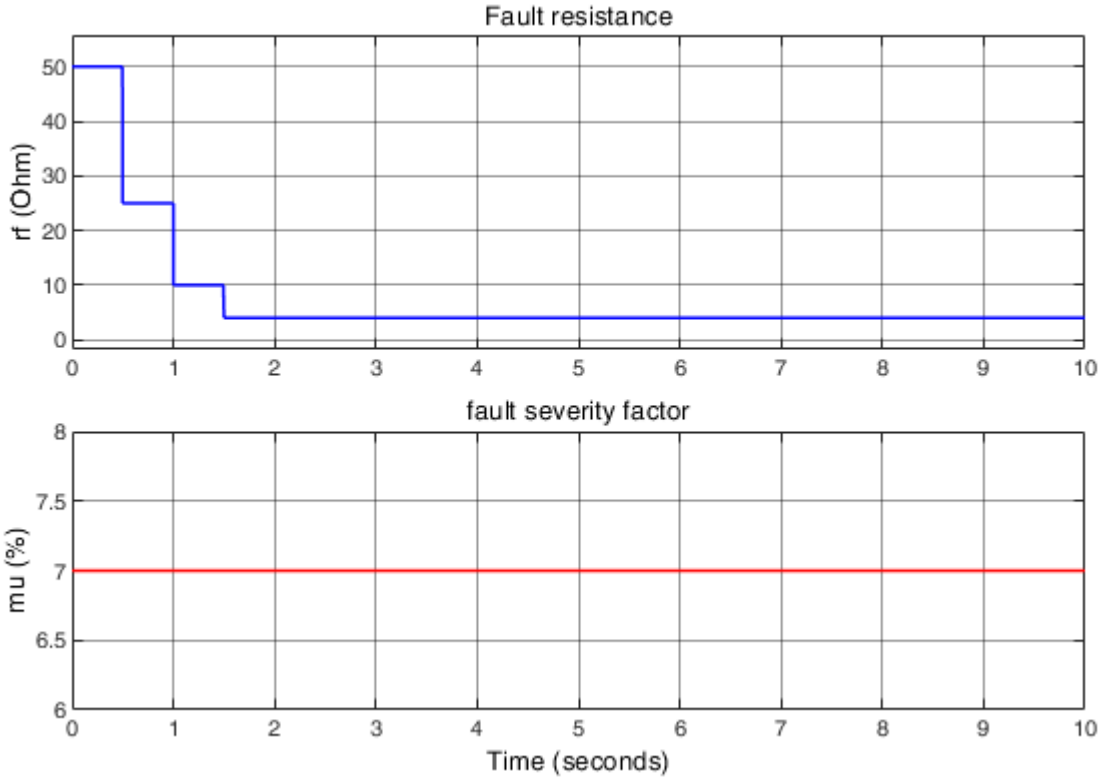

Fig. 9. Fault parameters development for Case 2.

It is assumed that the interturn fault degradation process is a monotonic trend then, becomes faster when fault severity is higher. Two cases of fault degradation process are studied in this paper: Case 1 the fault severity factor is set to the value of μ = 4% and r_f

decreases to lower values. Case 2 the fault severity factor is set to the value of μ = 7% and r_f decreases to lower values. Fig. 8 and Fig. 9 illustrate the former and later cases, respectively. In both cases, the fault is commenced with r_f = 50 Ω.

5.2.1 States, parameter estimation and fault indicator

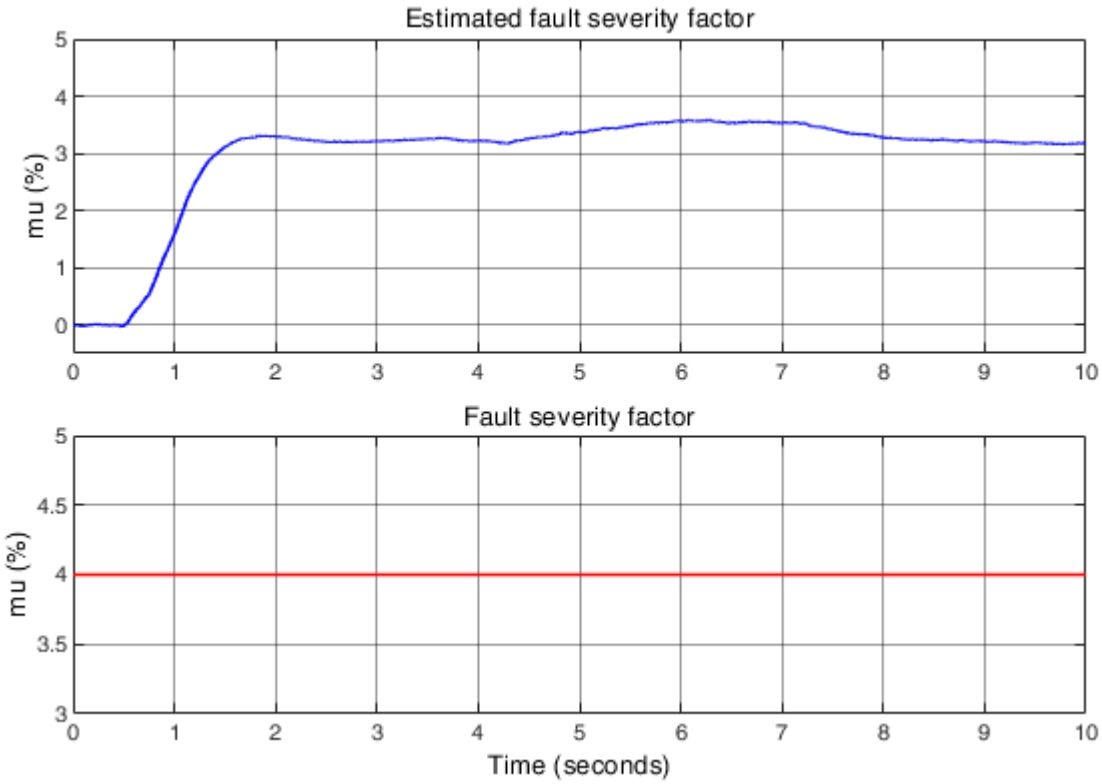

Fig. 10. Fault severity factor for Case 1.

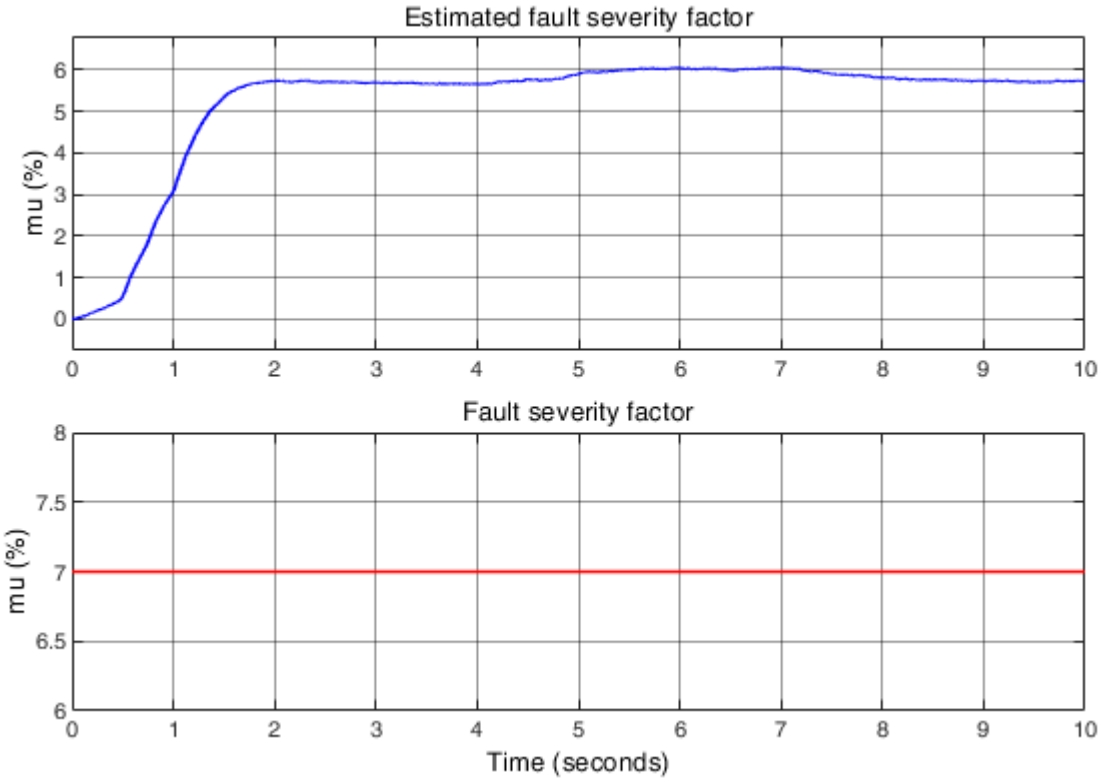

Fig. 11. Fault severity factor for Case 2.

In order to test the fault detection technique, the simulated states and parameter are compared with their estimated value through as shown in Fig. 10-15, for Case 1 and Case 2, respectively.

Fig. 10 and Fig. 11 show the simulation results of the estimation of the fault severity factor μ. The simulations results are accurate. The highest error is about 1.5%, but it is acceptable because this fault parameter value are corresponding to very low fault severity level. In addition the EKF estimator take account the disturbances of measured voltage and current in the estimation algorithm which is more practical in real scenario.

Fig. 12 and Fig. 13 show the simulated and estimated complete fault signal $\frac{2}{3}\mu i_f$ for Case 1 and for Case 2 respectively. The estimated complete fault signal closely matches with the simulated values. In addition we can see that the value of the complete fault current increases when the fault resistance decreases, and when the fault severity factor becomes severe.

Fig. 14 and Fig. 15 show the simulated and estimated ψ_{ds} for Case 1 and for Case 2 respectively. The estimated d-axis flux closely matches with the simulated values. Also, it can be observed that the inter turn fault has not an effect on the d-axis flux. Hence the fault indicator depends only of the fault parameters of the motor.

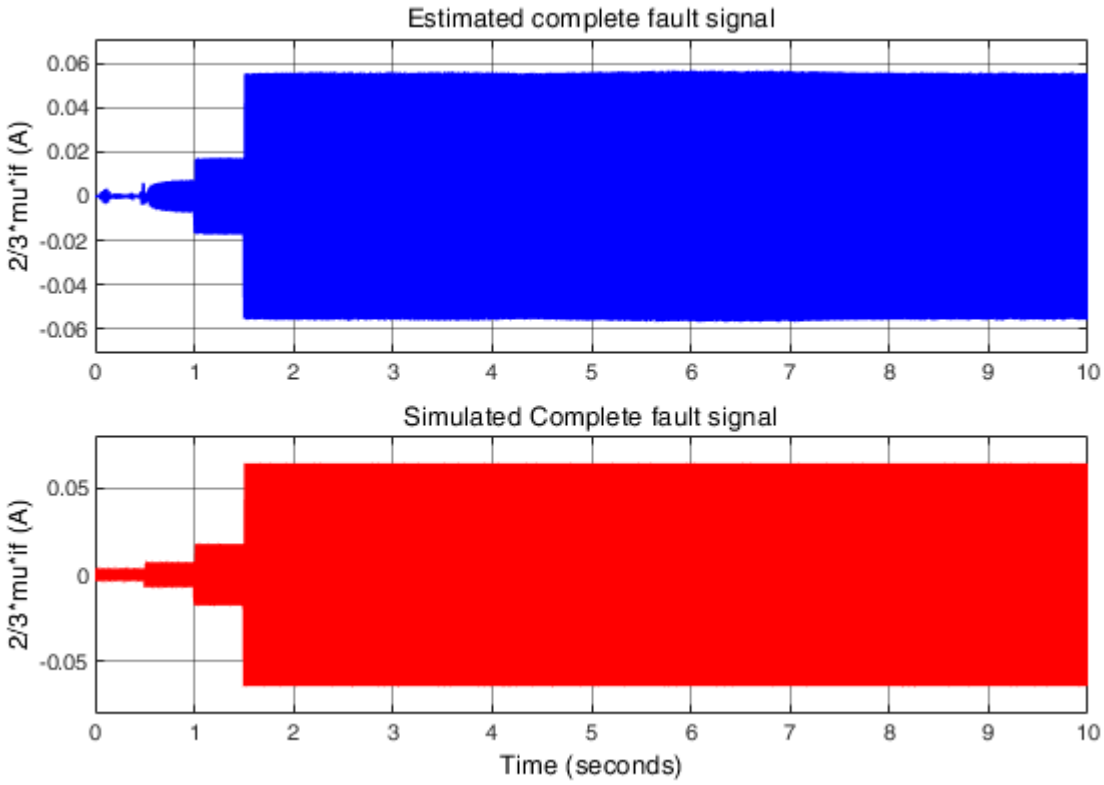

Fig. 12. Complete fault signal for Case 1.

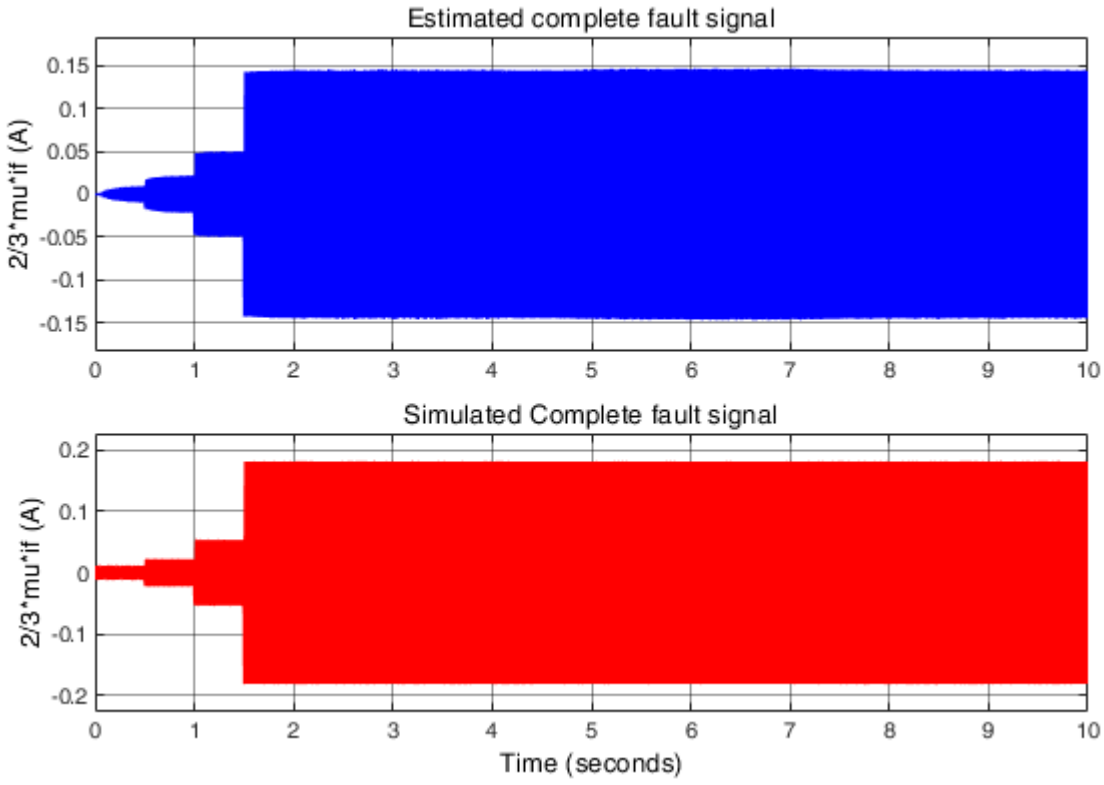

Fig. 13. Complete fault signal for Case 2.

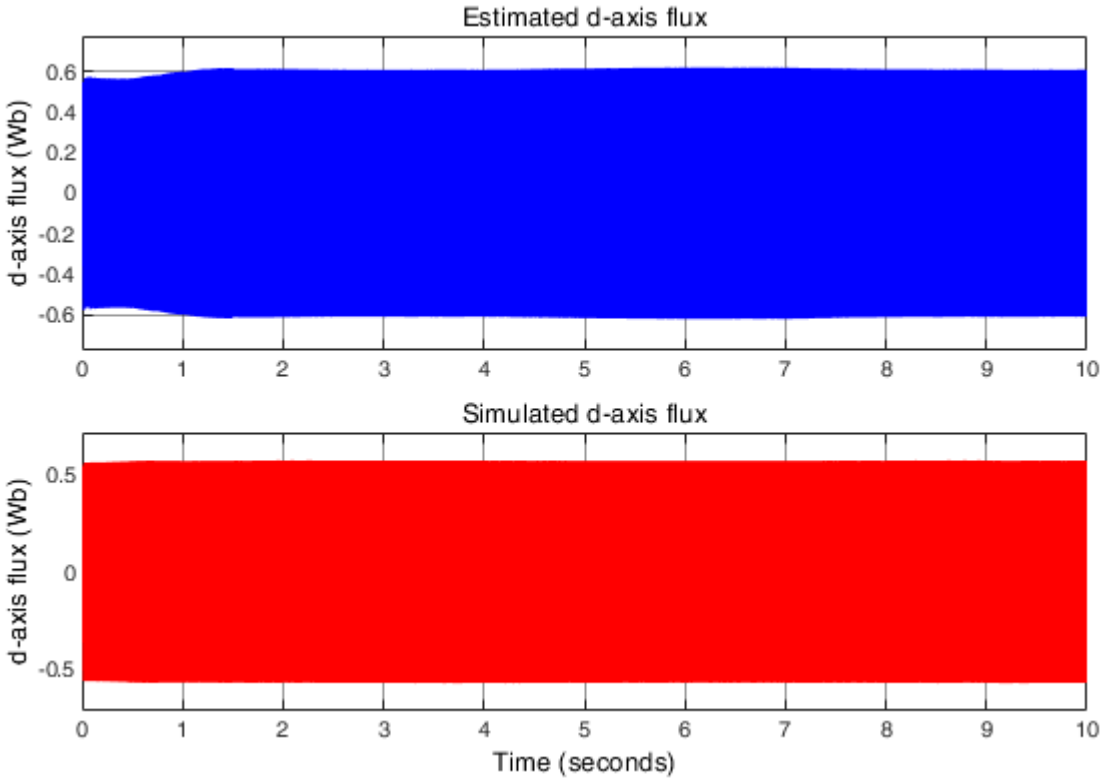

Fig. 14. D-axis flux for Case 2.

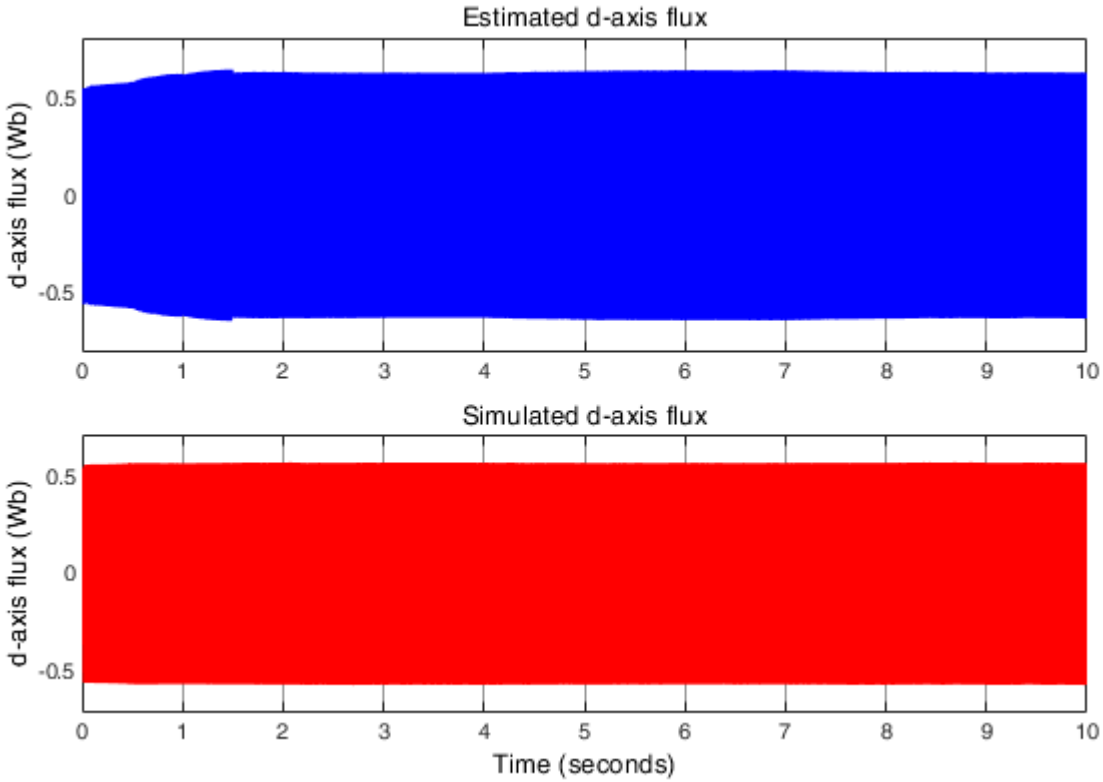

Fig. 15. D-axis flux for Case 2.

Hence, from Figs. 10 to 15, it can be concluded that the developed EKF state estimation technique is able to estimate the states and fault parameter of the motor accurately.

Fig. 16 and Fig. 17 show the evolution of the fault indicator for Case 1 and Case 2 respectively. In healthy case (when fault resistance is higher), the indicator remains close to 0, reflecting a good estimation of the theoretical electrical parameters. As the fault loop current increase when the fault resistance decrease, the fault indicator follows the trend of the complete fault signal. When the fault becomes severe (e.g. the fault severity factor is higher), the indicator increases with the number of short-circuited turns, which confirms that the fault detection is trickiest for a low number of short-circuited turns.

This study confirms that a threshold on this indicator can be used to make a quick and robust (against transient operation) fault decision.

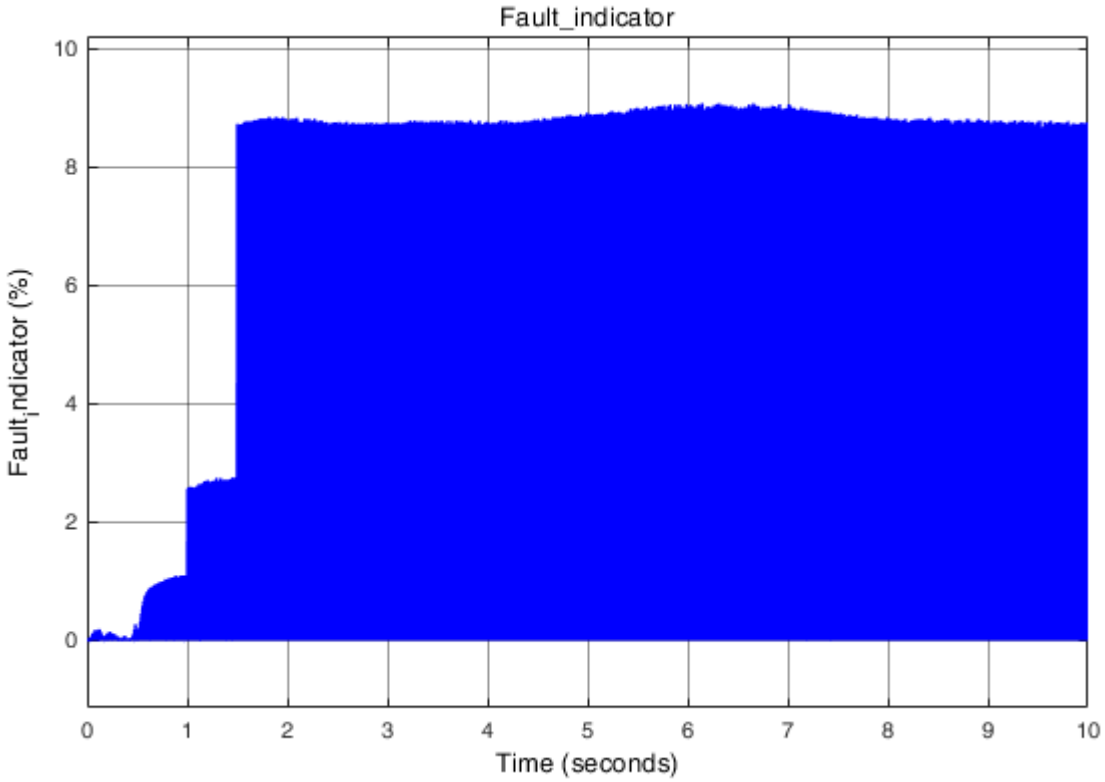

Fig. 16. Fault indicator for Case 2.

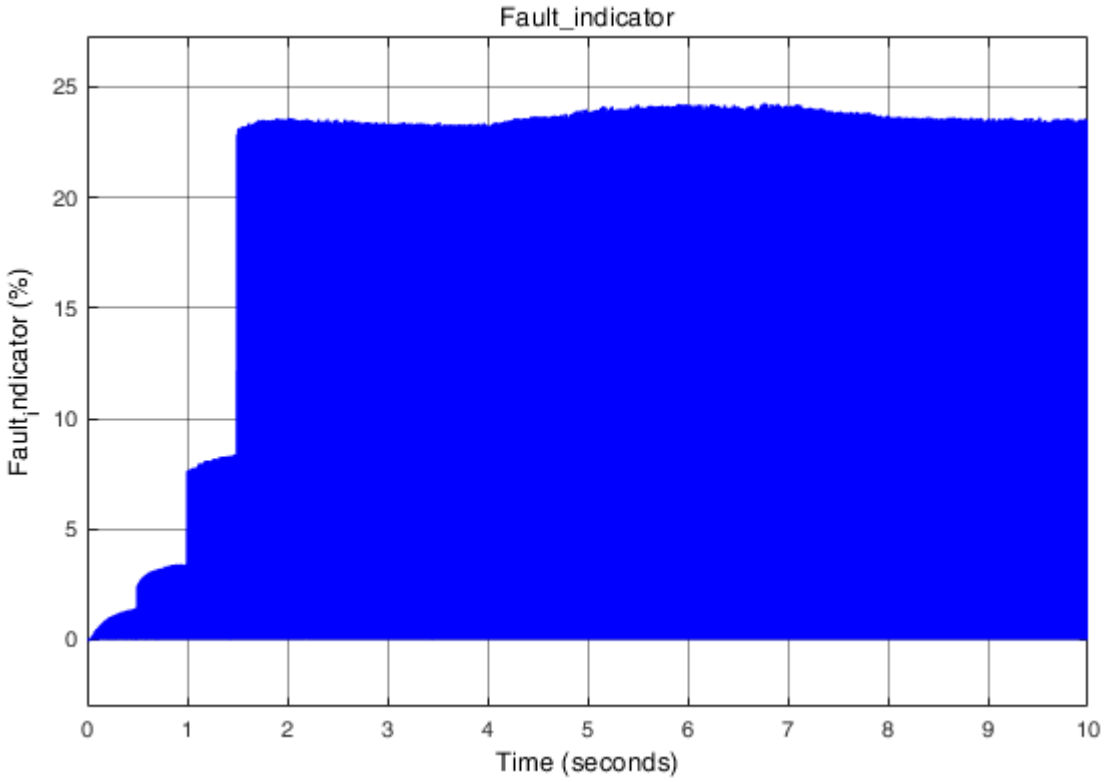

Fig. 17. Fault indicator for Case 2.

5.2.2 Fault compensation

As can be seen from the previous section, the fault detection block calculates the fault indicator, compares it to a defined threshold, and gives the decision to estimate the stator resistance using the fault severity factor. Once the stator is estimated, this value is fed to the DTC drive to update the parameter of it control algorithm.

Fig. 18 and 19 depict the simulation results describing the working of the fault tolerant control of DTC induction motor drive under stator inter turn fault with a fault severity factor μ = 7%. We can see that when the fault becomes severe, the stator current becomes unbalanced caused by the fault loop current. In addition, the value of the torque increase with an amplification of the torque oscillation. The amplification of the torque oscillation is caused by the control system of the DTC induction motor drive as seen in the section 3.3. Hence, the control system of the DTC drive acts as an amplifier of the torque oscillations primarily caused by the stator fault.

The fault tolerant control shows that the drive performance is affected by stator resistance variation and, estimate the true value of stator resistance is necessary to preserve and maintain the drive control performance.

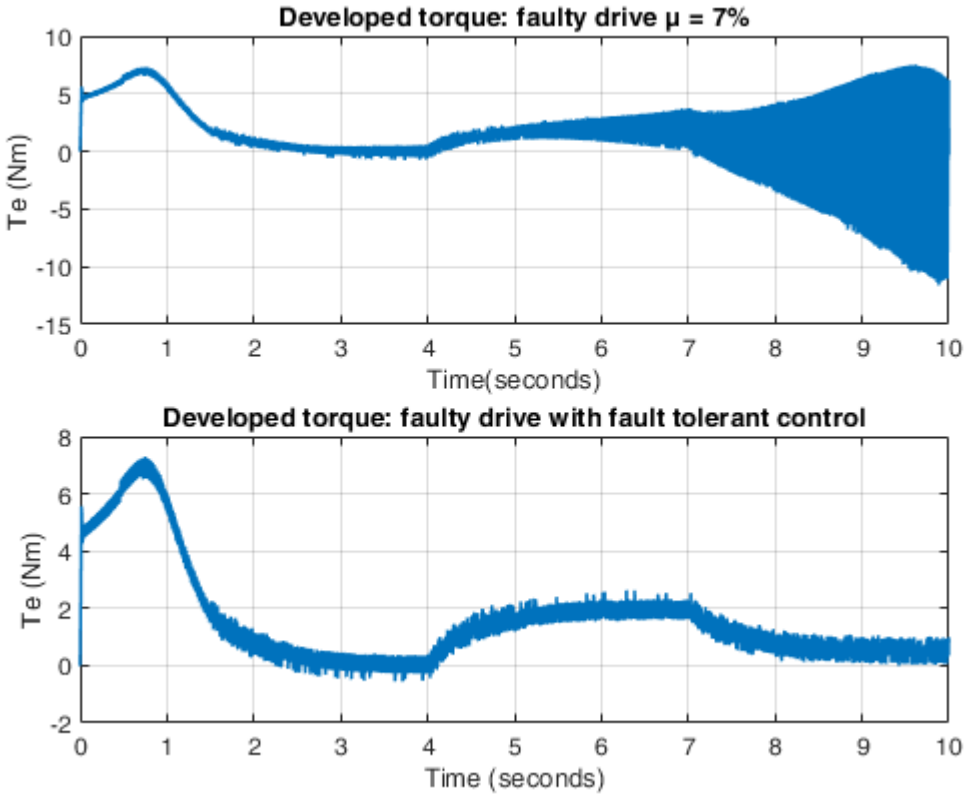

Fig. 18. Developed torque under faulty condition.

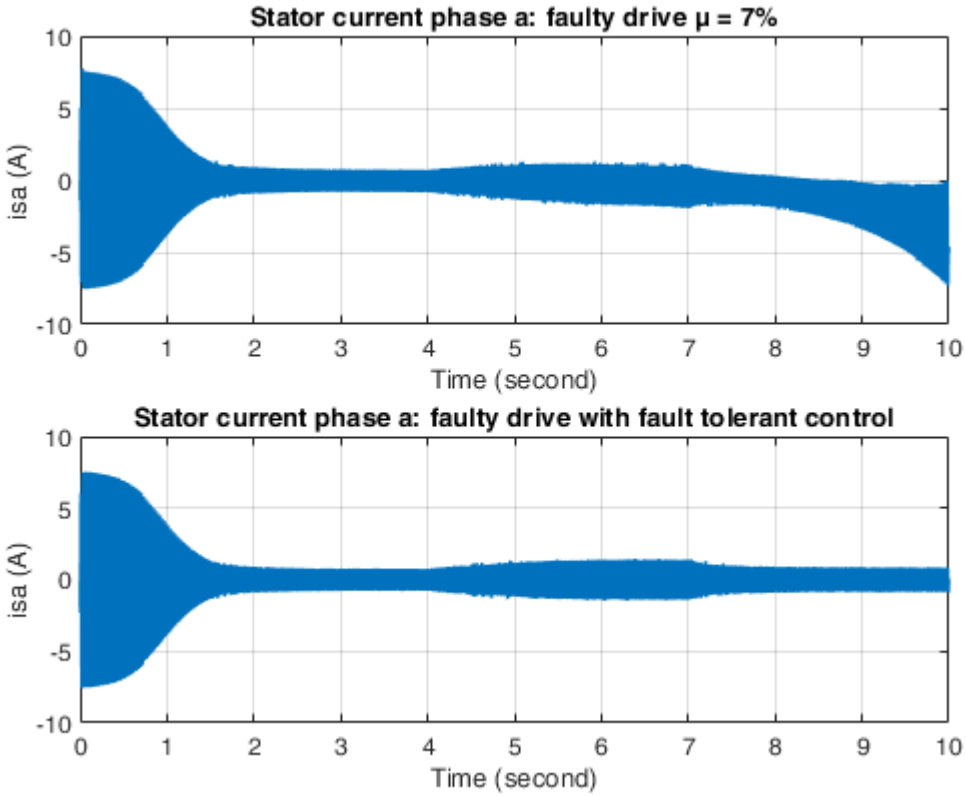

Fig. 19. Stator current under faulty condition.

6 Conclusion

This paper deals with fault detection and fault tolerant control for stator inter turn fault in DTC induction motor drives. For detecting the fault, a new fault detection technique was employed. By estimating the parameters which produce the torque oscillation due to a stator inter turn fault, a new fault indicator was calculated and the fault detection system can detect inter turn fault at incipient stage. In the moment of fault, the fault tolerant system is automatically activated, and estimate the true value of the stator resistance. This value is then fed to the DTC drive to update it parameter that allow to continue the drive uninterrupted system. The model is presented is the paper and the simulation results ensure the satisfactory operation of the proposed fault detection and tolerance system.

Table I: Parameters and nameplate of the induction motor [21]

Param.	Value	Param.	Value	Rating	Value	Rating	Value
L_{ls}	$32.1\ 10^{-3}\ H$	R_s	$9.292\ \Omega$	P_r	$746\ W$	PF	0.8
L_{lr}	$37.0\ 10^{-3}\ H$	R_r	$7.231\ \Omega$	V_r	$460\ V$	Pole pair	2
L_m	$0.895\ H$	J_m	$0.053\ Kgm^2$	I_r	$1.47\ A$	n_r	$1730\ rpm$

References

[1] https://ieeexplore.ieee.org/document/4658998

[2] https://ieeexplore.ieee.org/document/4658998

[3] https://ieeexplore.ieee.org/document/1495533

[4] https://ieeexplore.ieee.org/document/4752772

[5] https://ieeexplore.ieee.org/document/7392113

[6] https://www.mdpi.com/1996-1073/11/3/653

[7] https://ieeexplore.ieee.org/document/4025558

[8] http://www.diagnostyka.net.pl/INDUCTION-MOTOR-WINDINGS-FAULTS-DETECTION-USING-FLUX-ERROR-BASED-ESTIMATORS,109092,0,2.html

[9] https://www.mdpi.com/1996-1073/12/8/1507/pdf-vor

[10] https://ieeexplore.ieee.org/document/8445282

[11] https://ieeexplore.ieee.org/document/7993259

[12] https://ieeexplore.ieee.org/document/7793055

[13] https://ieeexplore.ieee.org/document/7390266

[14] https://ieeexplore.ieee.org/document/6980619

[15] http://ieeexplore.ieee.org/iel5/8893/28117/01257724.pdf

[16] https://ieeexplore.ieee.org/document/4025558

[17] https://ieeexplore.ieee.org/document/8388249

[18] https://ieeexplore.ieee.org/document/6980619

[19] https://ieeexplore.ieee.org/document/1003411

[20] http://ieeexplore.ieee.org/iel5/8893/28117/01257724.pdf

[21] https://ieeexplore.ieee.org/abstract/document/8338140/

[22] https://ieeexplore.ieee.org/document/6750029

[23] https://ieeexplore.ieee.org/document/8832252/

[24] https://ieeexplore.ieee.org/abstract/document/8721967/

[25] https://ieeexplore.ieee.org/document/7309182

[26] https://ieeexplore.ieee.org/iel5/41/4387790/06400245.pdf

[27] https://ieeexplore.ieee.org/document/7792962

List of Figures

Revision history

Rev.	Chapter	Description of change	Date	Name
0	All	Document release	15.11.2010	